King Saud University

Arabian Journal of Chemistry

www.ksu.edu.sa
www.sciencedirect.com

ORIGINAL ARTICLE

Discovery of novel indene-based hybrids as breast cancer inhibitors targeting Hsp90: Synthesis, bio-evaluation and molecular docking study

Amal M. Alosaimy [a], Amr S. Abouzied [b,c], Amani M. R. Alsaedi [d], Ahmed Alafnan [e], Abdulwahab Alamri [e], Mubarak A. Alamri [f], Mohammed Khaled Bin Break [b], Rehab Sabour [g], Thoraya A. Farghaly [h,*]

[a] *Department of Chemistry, Faculty of Applied Science, Umm Al-Qura University, Makkah Almukaramah, Saudi Arabia*
[b] *Department of Pharmaceutical Chemistry, College of Pharmacy, University of Hail, Hail 81442, Saudi Arabia*
[c] *Department of Pharmaceutical Chemistry, National Organization for Drug Control and Research (NODCAR), Giza 12553, Egypt*
[d] *Department of Chemistry, Collage of Science, Taif University, P. O. Box 11099, Taif 21944, Saudi Arabia*
[e] *Department of pharmacology and toxicology, college of pharmacy, University of Hail, Hail, Saudi Arabia*
[f] *Department of Pharmaceutical Chemistry, College of Pharmacy, Prince Sattam Bin Abdulaziz University, 11323, Alkarj, Saudi Arabi*
[g] *Department of Pharmaceutical Chemistry, Faculty of Pharmacy (Girls), Al-Azhar University, Cairo, Egypt*
[h] *Department of Chemistry, Faculty of Science, Cairo University, Giza 12613, Egypt*

Abstract Inhibition of Heat-shock protein 90 (Hsp90) is considered an attractive route in fighting against cancer proliferation. Herein, new indene derivatives targeting Hsp90 were synthesized, and biologically evaluated. The new series of indeno-pyrimidine and indeno-pyridine were synthesized from the reaction of indene-enaminone with various heterocyclic amines and active methylene derivatives. Two breast cancer cell lines were used to examine the new compounds *in vitro* for their anticancer activity, namely, MCF-7 and MDA-MB231 cancer cells. The new indene derivatives **8a-c**, **17a**, and **25** displayed significant antitumor effect especially on MCF-7 cell line compared to doxorubicin. Derivative **8a** was further subjected to Hsp90 enzyme assay aiming to ensure the inhibitory potential of such compound on Hsp90, it displayed IC$_{50}$ = 18.79 ± 0.68 nM relative to Alvespimycin as a reference drug. Finally, molecular modeling of the most active compounds in

* Corresponding author.
 E-mail addresses: thoraya-f@hotmail.com, thoraya-f@cu.edu.eg (T.A. Farghaly).
Peer review under responsibility of King Saud University.

Production and hosting by Elsevier

the Hsp90 binding site was done presenting agreement with the *in vitro* anti-Hsp90 activity.

1. Introduction

Heat shock protein 90 (Hsp90) is a molecular chaperone that is a member of the heat shock protein family and plays an important role in cell's vital processes including cell growth, differentiation, and survival (Whitesell and Lindquist, 2005; Taipale et al., 2010; Biebl and Buchner, 2019). Consequently, inhibiting Hsp90 might cause cancer cells to collapse or become much weaker (Neckers and Mollapour, 2015; Zhang, et al., 2021). Breast cancer is still the most commonly diagnosed malignancy in women and the second biggest cause of cancer-related fatalities. Despite continued efforts to find novel therapies, breast cancer mortality rates have just lately begun to fall, and this is most likely due to early detection of the disease (Berry et al., 2005). However, it was reported that inhibiting Hsp90 causes client proteins to degrade, resulting in inhibition of both cancer cell growth and proliferation, especially those proteins related to breast cancer which account for about 20 % of breast cancers and have violent clinical aspects, leading to poor diagnosis and clinical consequences, therefore high expression of Hsp90 is correlated with high expression of these client protiens, such correlation makes targeting Hsp90 a considerable approach to overcome breast cancer (Nguyen et al., 2021). Hsp90′s therapeutic potential is also increased by the fact that cancer cells express it 2–10 times more than normal, healthy cells do. Targeting Hsp90 can also get around the well-known cancer resistance problem due to its potential for affecting numerous oncogenic protein pathways (El-Shafey et al., 2020; Lianos et al., 2015). Therefore, Hsp90 has consequently become a desirable and focused target for the development of new medications (Gimenez Ortiz and Montalar Salcedo, 2010; Liu et al., 2022). Hsp90 inhibitors include a number of natural products and their derivatives as well as fully synthetic com-
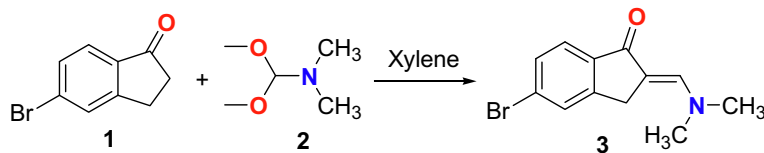
Scheme 1   The synthesis of enaminone derivative **3**.
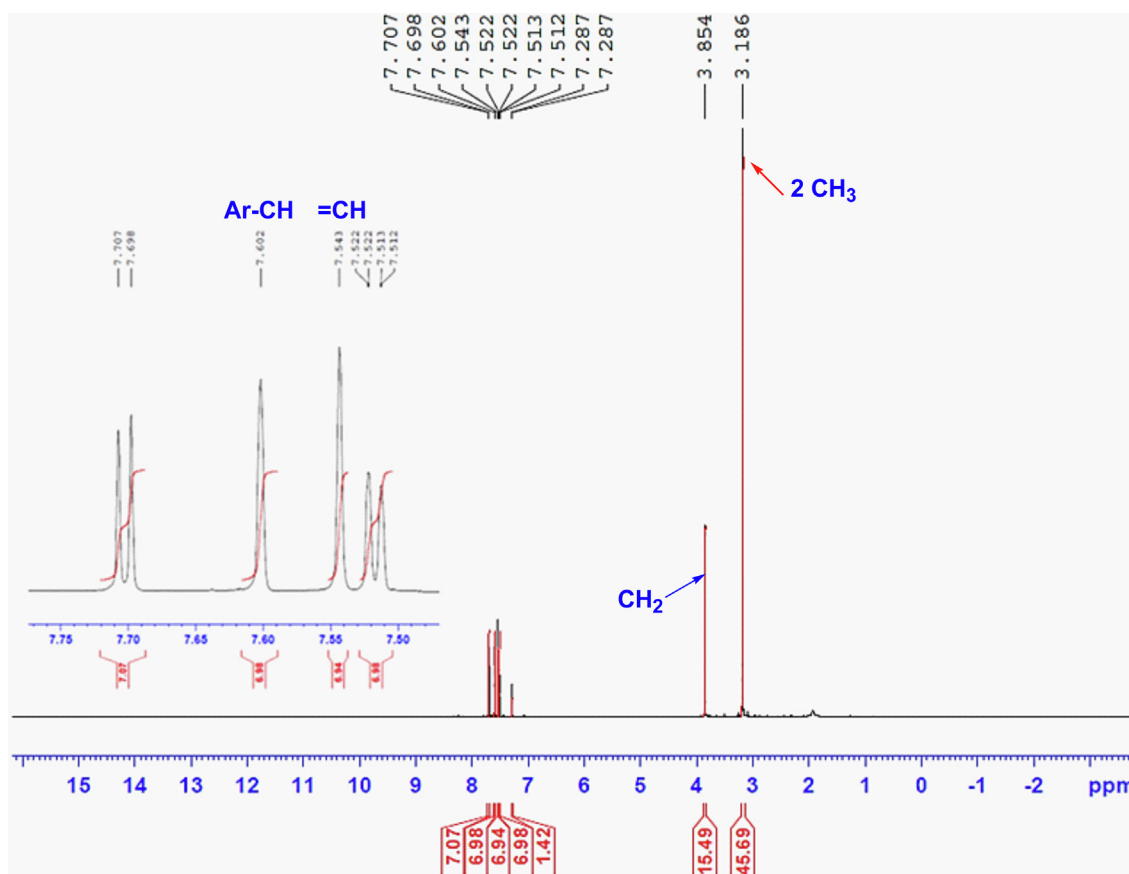
Fig. 1   The ^{1}H NMR spectrum of enaminone derivative **3** in CDCl$_3$.

pounds (Li et al., 2020). A new selective Hsp90 inhibitor called Pimite-spib recently demonstrated therapeutic activity in patients with advanced gastrointestinal stromal tumors resistant to conventional therapies (Sheridan, M. H., 2022; Akira et al., 2022).

Different indene derivatives were reported as analogues of Hsp90 inhibitors exerting marked inhibitory effect on Hsp90 with cytotoxic effect on different cell lines (Chaudhury et al., 2021). Fusion between indene scaffold and nitrogen bearing moiety was reported and such hybrid proved marked antiproliferative effect against different cancer cell lines, where some new derivatives displayed marked effect espe-

cially against MCF-7 breast cancer cell line (Fayed et al., 2020). Because of their chemical and biological relevance, indeno-pyrimidines have been investigated. They have been discovered to have numerous pharmacological characteristics, including antitumor effect. A large number of structurally new indeno-pyrimidines were shown to exhibit significant anticancer effect both *in vitro* and *in vivo* (Ghorab and Alsaid, 2015). Besides, Indeno-pyridines have been reported for their anticancer activity especially against breast cancer cell line (MCF7) (Ghorab and Alsaid, 2012). Concerning pyrimidine scaffold, the anticancer action of pyrimidine derivatives has been described

Ar: a, Ph; b, 4-ClC$_6$H$_4$; c, 3-ClC$_6$H$_4$; d, 2-NO$_2$C$_6$H$_4$
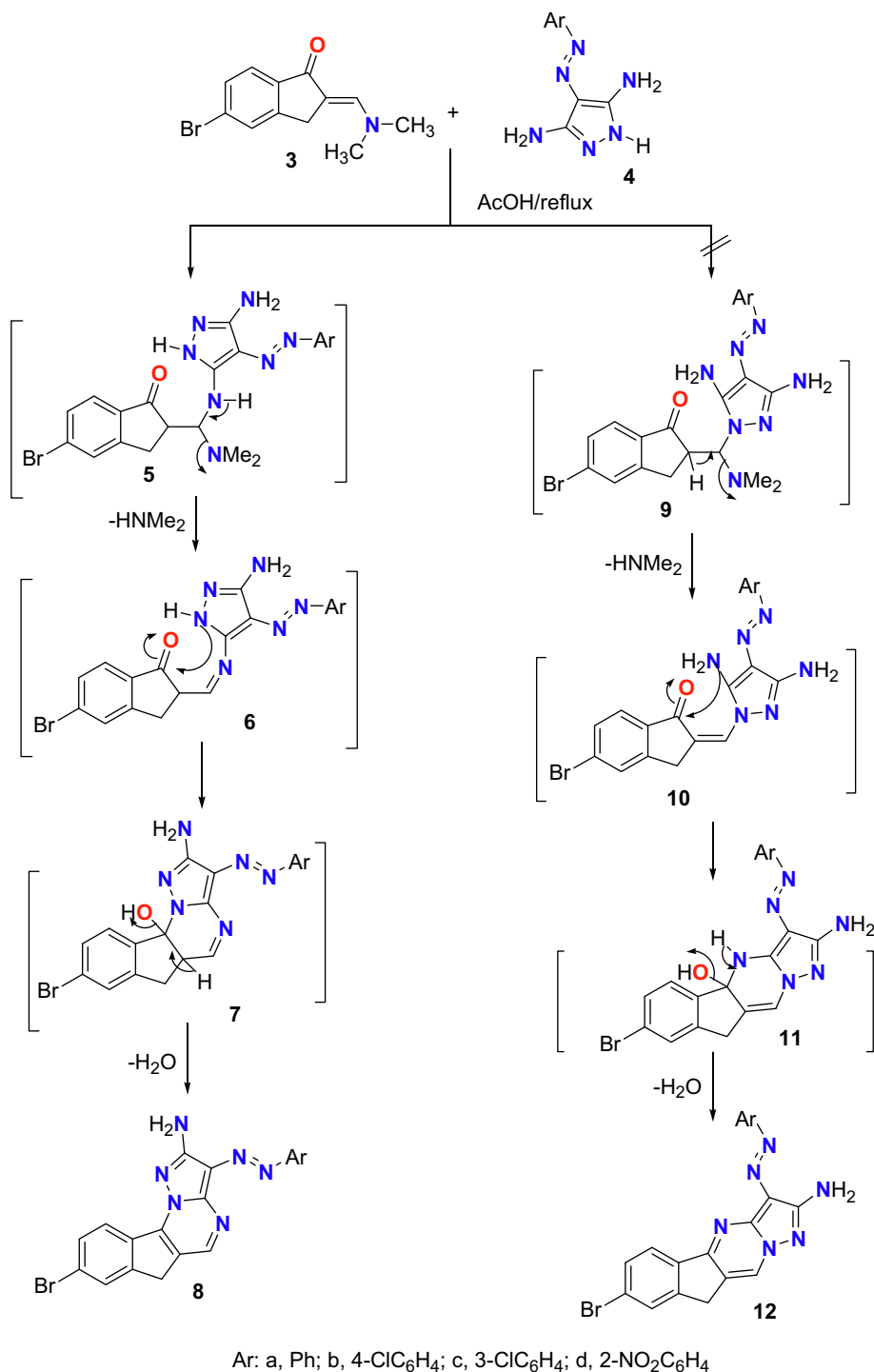
Scheme 2 Reaction of enaminone **3** with heterocyclic amines **4**.

through a number of mechanisms, among which is the inhibition of Hsp90 enzyme (Davies et al., 2012). Interestingly, fused pyrimidines such as pyrazolo-pyrimidine, triazolo-pyrimidine and benzimidazole-pyrimidine showed significant anti-MCF-7 activity (Aastha et al., 2021). From our experience over 20 years to design and synthesis of biologically active heterocyclic derivatives (Alsaedi et al., 2022; Abbas et al., 2022; Alamri et al., 2023; Almehmadi et al., 2021; Farghaly et al., 2015, 2021; Althagafi et al., 2019; Bayazeed et al., 2022), we decided to utilize the indeno-pyrimidine scaffold in the synthesis of new derivatives, and examine their anticancer activities especially against breast cancer cell lines.

2. Results and discussion

Herein, our project was directed to synthesize novel series of indeno-pyrimidines or indeno-pyridine moieties *via* the reaction of 5-bromo-2-dimethylaminomethylene-indan-1-one with heterocyclic amines and active methylene derivatives. Such project started with the synthesis of enaminone **3** through the condensation of indanone derivative **1** with DMF-DMA in dry xylene as illustrated in Scheme 1. The structural identity of the novel enaminone derivative **3** was confirmed by various spectroscopic analyses. The ^{1}H NMR spectrum of enaminone derivative **3** (Fig. 1) revealed three characteristic singlet signals for the two CH_3 of $N(CH_3)_2$, the CH_2 and $=CH$ groups at δH: 3.19, 3.85 and 7.54 ppm in addition to the remarkable signals for three protons of aromatic ring. Also, the ^{13}C NMR showed characteristic carbon signals for the two chemically equivalent two methyl groups of $N(CH_3)_2$ and $C=O$ groups at δC: 31.1 and 191.0 ppm, respectively.

The second step in the synthesis of a series of indanopyrimidine is the reaction of enaminone derivative **3** with 3,5-diamino-4-arylazopyrazoles **4a-d** in acetic acid as depicted in Scheme 2. This reaction proceeded through the formation of three intermediates **5–7** to form four derivatives of indeno [2,1-*e*]pyrazolo[1,5-*a*]pyrimidin-2-amine **8a-d**. The other products **12a-d** with their intermediates **9–11** were discarded based on the previous fact that proofed using X-ray single crystal analyses (Farghaly et al., 2010), that the reaction between exocyclic-enaminone and heteroamine derivatives proceeded *via* at first the addition of exocyclic amino group to the double bond of $=CH-N(Me)_2$ followed with elimination of $NH(Me)_2$ then cyclization through nucleophilic attack of the cyclic-NH to the carbon of C=O of the enaminone moiety with elimination of water molecule. The structure of indeno[2,1-*e*]pyrazolo[1,5-*a*]pyrimidin-2-amine derivatives **8a-d** was confirmed from interpretation of their IR, Mass, and NMR spectral data with the suggested structure. For example, the mass spectrum of derivative **8a** (Fig. 2) showed the exact molecular weight as well as several fragments corresponding to the fragmentation species of that derivative. In addition, the ^{1}H NMR of the same derivative **8a** showed the correct signals corresponding to 13 protons for CH_2 (3.60), NH_2 (7.25), Ar-H (7.35–8.01) and pyrimidine- H (8.54) ppm.

In the same way, the enaminone derivative **3** was reacted with another two derivatives of aminopyrazolone **13a,b** (Scheme 3) to afford the indeno[2,1-*e*]pyrazolo[1,5-*a*] pyrimidin-2(6*H*)-one derivatives **17a,b**. Such reaction was achieved through Michael type addition of NH_2 group to the double bond of enaminone moiety ($=CH-N(Me)_2$) with
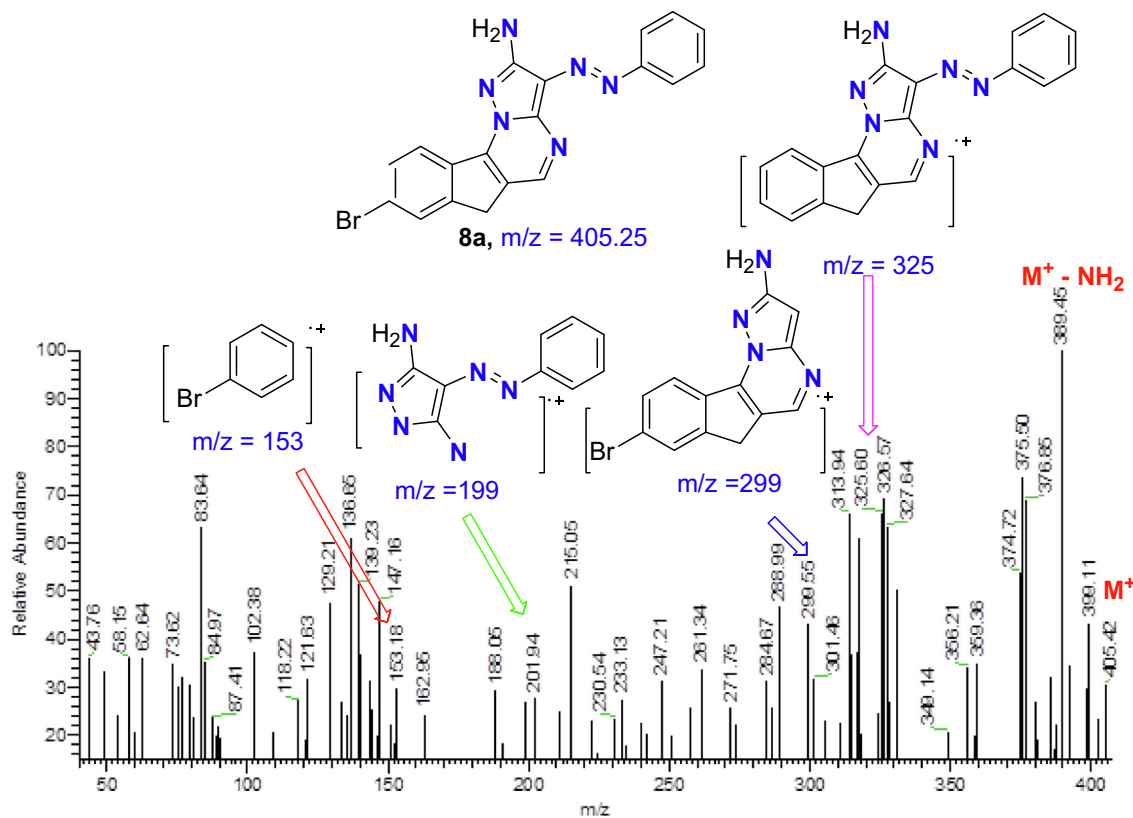
Fig. 2 The mass spectrum with fragmentation of derivative **8a**.
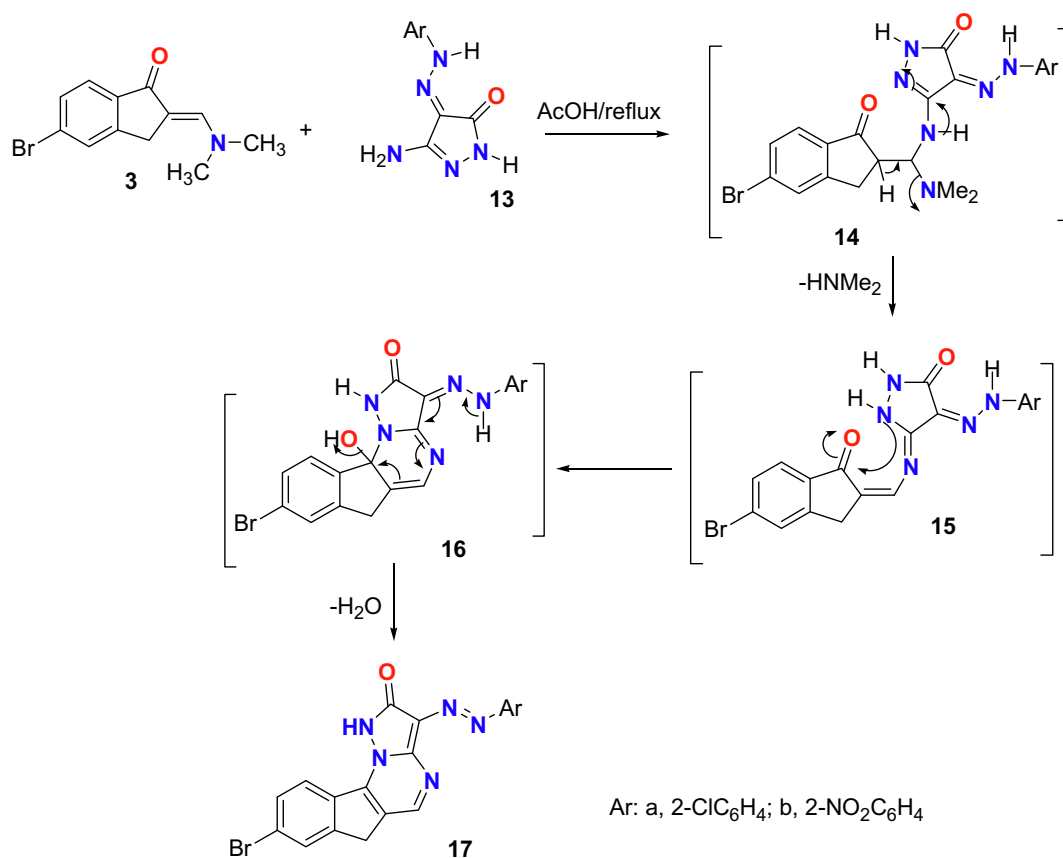
Scheme 3 Reaction of enaminone **3** with heterocyclic amines **13a,b.**

abstraction of NH(Me)$_2$ to afford the intermediate **15** followed by cyclization through nucleophilic attack of the cyclic NH to the carbonyl carbon with removal of H$_2$O molecule from intermediate **16**.

In Scheme 4, another two heteroamines **18** and **19** were reacted with the enaminone derivative **3** in refluxed acetic acid to give two indinopyrimidine derivatives fused with triazole ring **20** or benzimidazole **21**. The structure of the two products

was proved from their spectral data as illustrated in experimental section.

Recently published research has drawn our attention to the biological significance of the indeno[1,2-b]pyridine derivatives as anticancer (Kadayat et al., 2015, 2016), topoisomerase inhibitory (Shrestha et al., 2018; Kadayat et al., 2015), anti-aggression (Bell and Brown, 1979) and antimicrobial activities (Brahmbhatt, et al., 2015). From these reports we interested
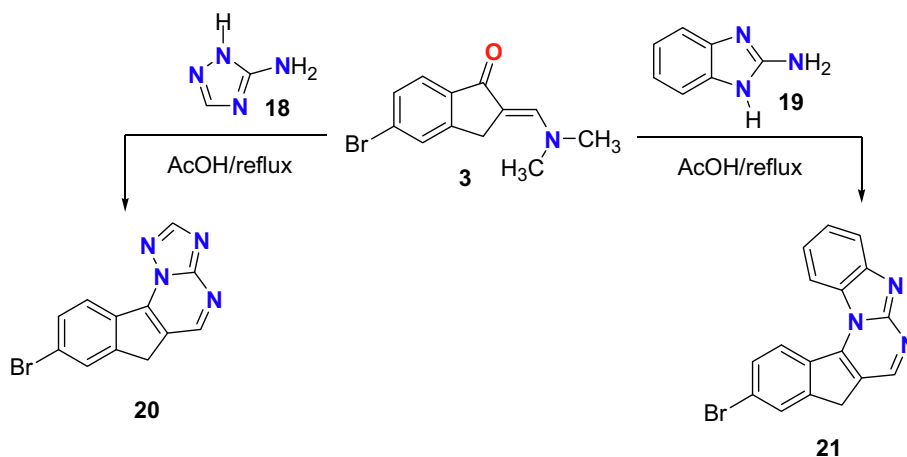
Scheme 4 Reaction of enaminone **3** with heterocyclic amines **18** and **19.**
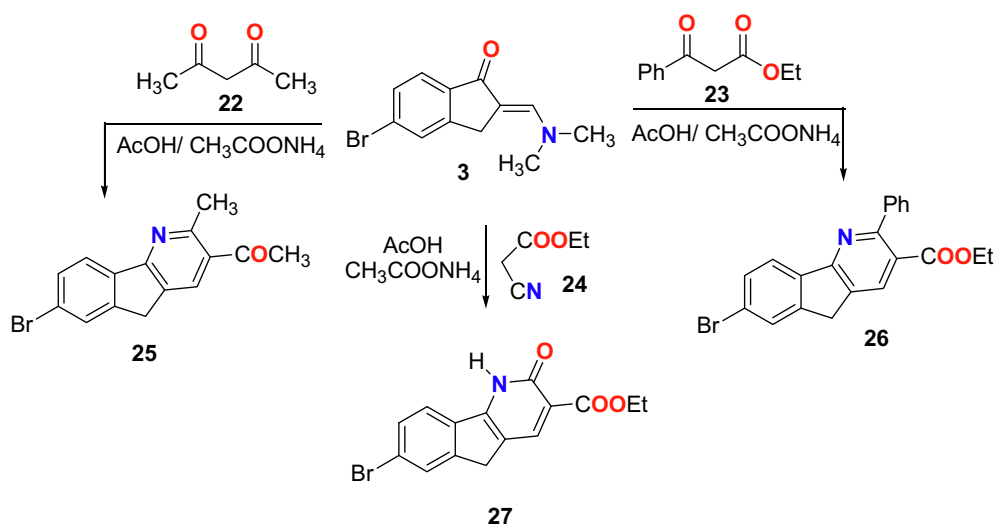
Scheme 5 Reaction of enaminone **3** with active methylene derivatives **22–24**.

herein to synthesize three new indeno[1,2-*b*]pyridine derivatives **25**, **26** and **27** from the reaction of enaminone derivative **3** with active methylene **22–24** in acetic acid and ammonium acetate under reflux (Scheme 5).

2.1. Biological activity

2.1.1. In-vitro cytotoxicity

In this study the cytotoxic impact of 12 novel compounds was investigated *in vitro* against two breast cancer cell lines (MCF7 and MDA-MB231) using the MTT assay. The IC_{50} values of such compounds were calculated as shown in Table 1. A well-known chemotherapeutic drug (doxorubicin) and Alvespimycin (17-DMAG) were used as reference drugs. 17-DMAG displayed potent activity against both tested cell lines with IC_{50} = 7.43 μM and 6.57 μM against both cell lines respectively. Compounds **8a-c**, **17a**, and **25** in general, showed

considerable cytotoxic activity against MCF7 revealing IC_{50} ranging from 26.44 to 39.62 μM. In particular, compound **8a** was the most active, comparing its cytotoxic effect against both cell lines relative to doxorubicin as a reference drug. From the obtained results, it is worth mentioning that all the tested compounds displayed lower activities against MDA-MB231 cancer cell line comparing to reference drug except compound **8a** among them showed IC_{50} = 69.95 μM exceeding that of doxorubicin having IC_{50} = 74.32 μM. Additionally, fusion of indene ring with nitrogen bearing heterocyclic rings markedly improved the activity especially against MCF7 cancer cell line as found in compound **3**, it exerted very low activity comparing with the reference drug, and yet marked improvement in cytotoxicity is recorded upon fusion.

It is observed that compounds **8a-c** bearing 2-amino and 3-phenyl diazenyl substituents on the pyrazolo[1,5-*a*]pyrimidine scaffold displayed significant inhibitory activities, where the un-substituted phenyl ring in **8a** exerted the highest activity against MCF7 with IC_{50} = 26.44 μM comparing with doxorubicin having IC_{50} = 31.16 μM. Introduction of electron with-

Table 1 The anticancer activity of indene derivatives **3, 8a-d, 17a, b, 20, 21** and **25–27** doxorubicin against MCF7, MDA-MB231.

Compound no.	IC_{50} (μM)	
	MCF7	MDA-MB231
3	> 100	> 100
8a	26.44 ± 4.47	69.95 ± 2.45
8b	37.01 ± 7.54	> 100
8c	39.62 ± 10.21	> 100
8d	> 100	> 100
17a	38.41 ± 4.30	> 100
17b	> 100	> 100
20	61.62 ± 2.34	93.58 ± 1.39
21	76.31 ± 2.61	88.85 ± 1.55
25	32.85 ± 3.97	> 100
26	> 100	> 100
27	> 100	78.52 ± 2.24
Doxorubicin	31.16 ± 3.43	74.32 ± 1.10
Alvespimycin (17-DMAG)	7.43 ± 1.02	6.57 ± 2.01

Data are expressed as the mean ± SD of three independent experiments.

Table 2 The cytotoxic effect of both **8a** and doxorubicin against WI-38 cells.

Compound	IC_{50} (μM) WI-38
8a	78.34 ± 2.33
Doxorubicin	66.15 ± 1.78

Data are expressed as the mean ± SD of three independent experiments.

Table 3 Inhibitory effect of compound **8a** on Hsp90 enzyme.

Compound	Hsp90 IC_{50} (nM)
8a	18.79 ± 0.68
Alvespimycin (17-DMAG)	62.00 ± 1.78

Data are expressed as the mean ± SD of three independent experiments.
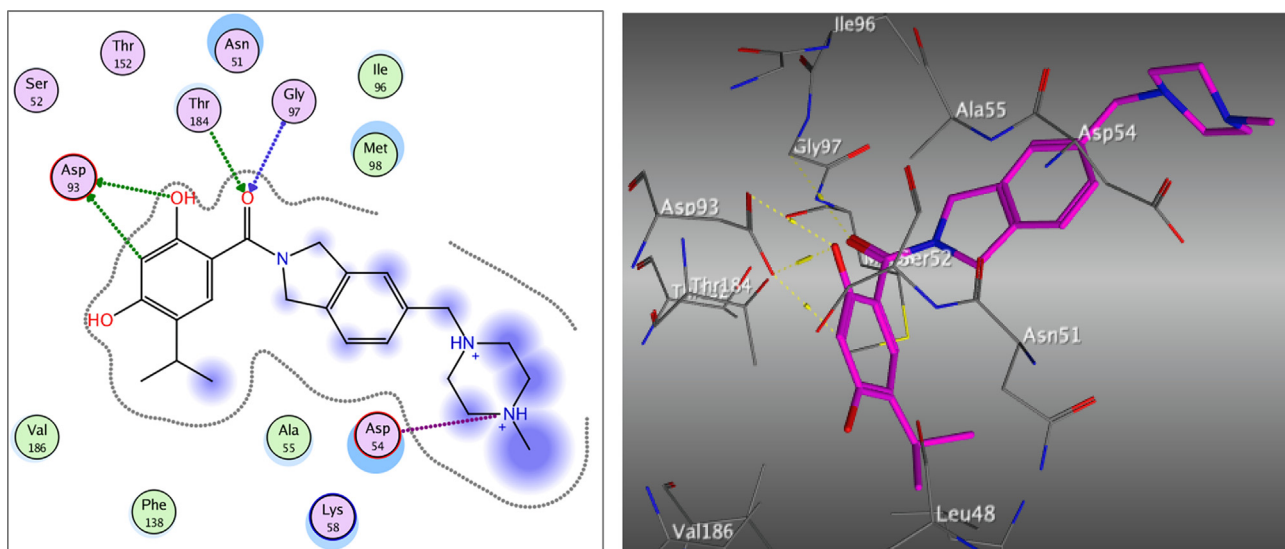
Fig. 3 The 2D and 3D proposed binding modes of the co-crystalized ligand inside Hsp90 receptor active site.

Table 4 The docking scores and binding interactions of the ligand, **8a-c**, **17a**, and **25**.

Compound	Docking score (Kcal/mol)	Interacting amino acids (Type of interaction)
8a	−8.556	Asp93, Gly97 (2H-bonds)
8b	−8.213	Asp93, Gly97 (2H-bonds)
8c	−7.982	Gly97 (1H-bond), His154 (pi-H)
17a	−8.651	Gly97 (3H-bonds)
25	−7.028	Asp93, Lys112 (2H-bonds), Asn51 (pi-H)
Ligand	−7.103	Asp54,Asp93, Gly97, Thr184 (5H-bonds)

drawing group in both para (p-Cl) and meta (m-Cl) positions of the phenyl ring in **8b** and **8c** respectively exerted lower inhibitory effects with IC_{50} = 37.01 and 39.62 μM respectively on MCF7 cancer cell line than the plain phenyl ring. Interestingly the presence of 2-C=O instead of 2-amino, and o-Cl phenyl diazenyl substituents retained a moderate activity as in **17a** revealing IC_{50} = 38.41 μM. Furthermore, marked drop-in activity was noticed upon introducing o-NO$_2$ group as in compounds **8d**, **17b**. On the other hand, both **20** and **21** displayed moderate activities against both tested cell lines. Regarding indeno-pyridine derivatives, the presence of a 2-CH$_3$ group on the pyridine ring as in compound **25** was significantly better in terms of activity compared to its counterparts **26**, **27** which held 2-phenyl and 2-C=O groups, respectively. The IC_{50} of compound **25** was 32.85 M, which was nearly equivalent to the reference drug.
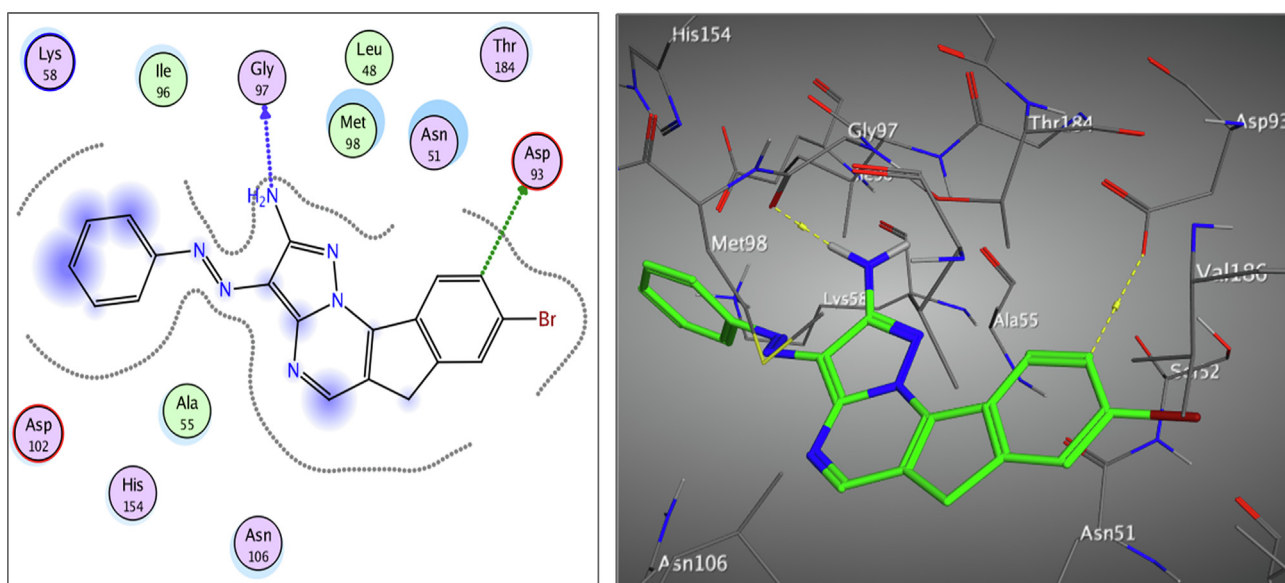
Fig. 4 The 2D and 3D proposed binding modes of **8a** inside Hsp90 receptor active site.

2.1.2. Effect on normal cells

The promising new compound **8a** was further assessed by examining its cytotoxicity against noncancerous normal cells (WI-38 cells), as presented in Table 2. From cytotoxicity results it was obvious that MCF-7 cell line was more sensitive than MDA-MB231. The obtained results showed that **8a** recorded IC$_{50}$ value = 78.34 ± 2.33 μM higher than that recorded against MCF-7 cell line and nearly equal to the corresponding IC$_{50}$ of MDA-MB231 cell line, Therefore selective toxicity should be improved before further development of such compound. Our promising new compound was further subjected to an examination of the possible anticancer mechanism of action.

2.1.3. Effect of target compound 8a on Hsp90 enzyme

The inhibitory effect of compound **8a** on Hsp90 enzyme was assessed *via* using the Hsp90 inhibitor Alvespimycin (17-

DMAG) as a reference drug. Consistent with the cytotoxicity results, compound **8a** revealed marked inhibitory effect on Hsp90 enzyme with IC$_{50}$ = 18.79 ± 0.68 nM exceeding that of the reference drug as presented in Table 3.

2.2. Molecular modeling inside the active binding site of Hsp90

In order to perform molecular docking of the most active compounds (**8a-c**, **17a**, and **25**) revealing the highest activity against MCF7 cancer cells, especially compound **8a** with *in vitro* inhibitory effect on Hsp90 enzyme, we utilized MOE 2014.0901 [33] aiming to find a possible fitting inside the Hsp90 reported active site. Molecular modeling inside the active binding site of Hsp90 was performed on the crystal structure of Hsp90 downloaded from the protein data bank (PDB: 2xjx) (Woodhead, et al., 2010). The most important amino acids in the active site which are considered the con-
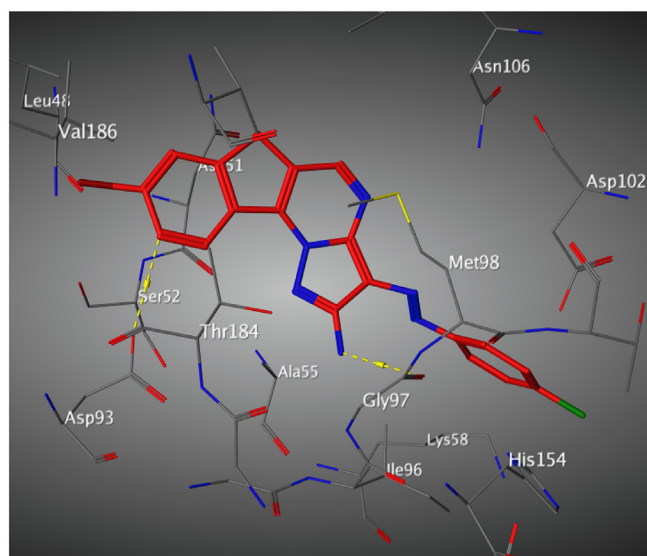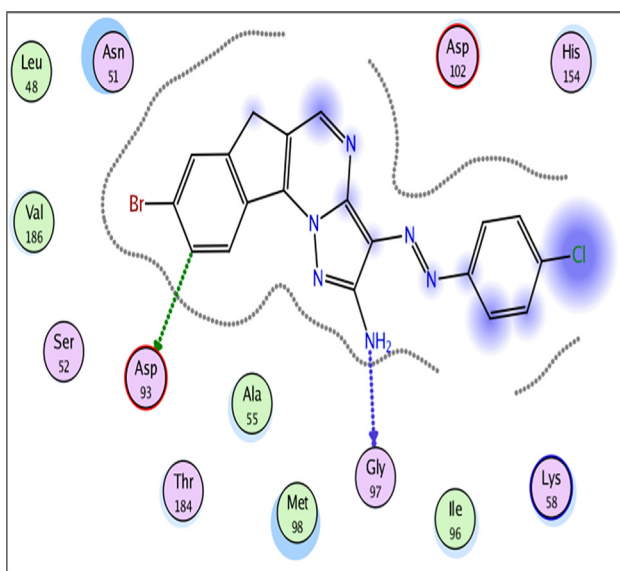
Fig. 5 The 2D and 3D proposed binding modes of **8b** inside Hsp90 receptor active site.
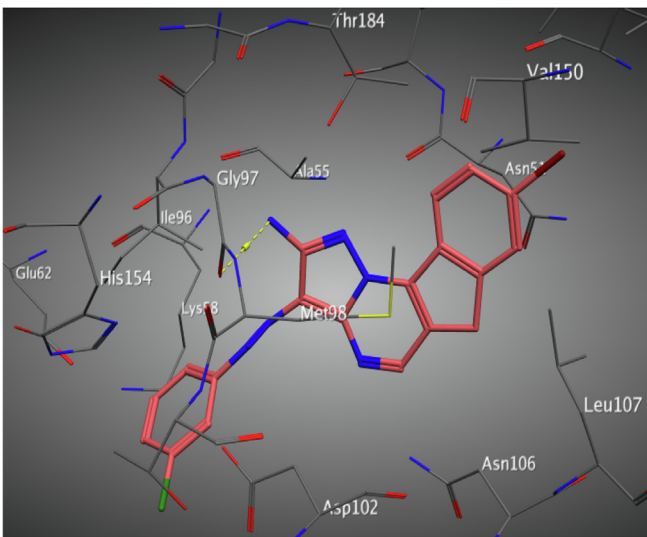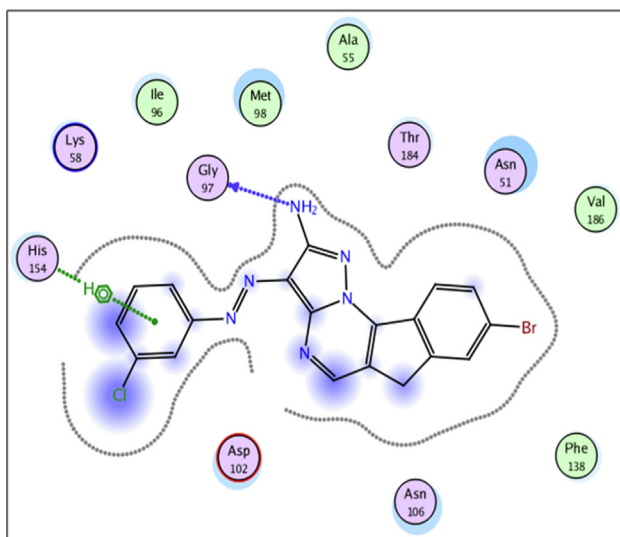
Fig. 6 The 2D and 3D proposed binding modes of **8c** inside Hsp90 receptor active sit.
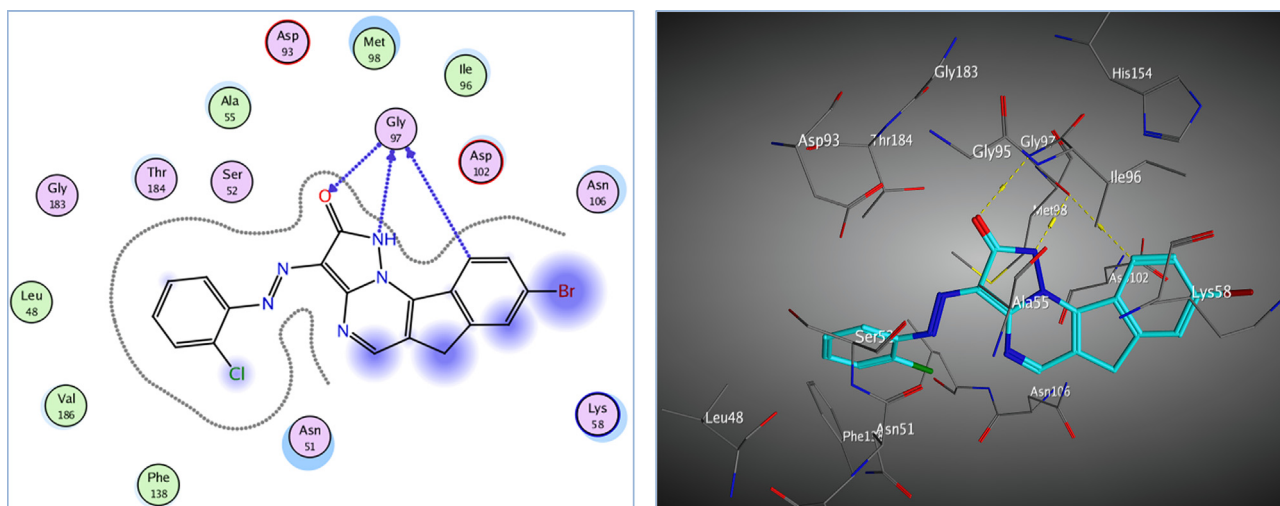
Fig. 7 The 2D and 3D proposed binding modes of **17a** inside Hsp90 receptor active site.
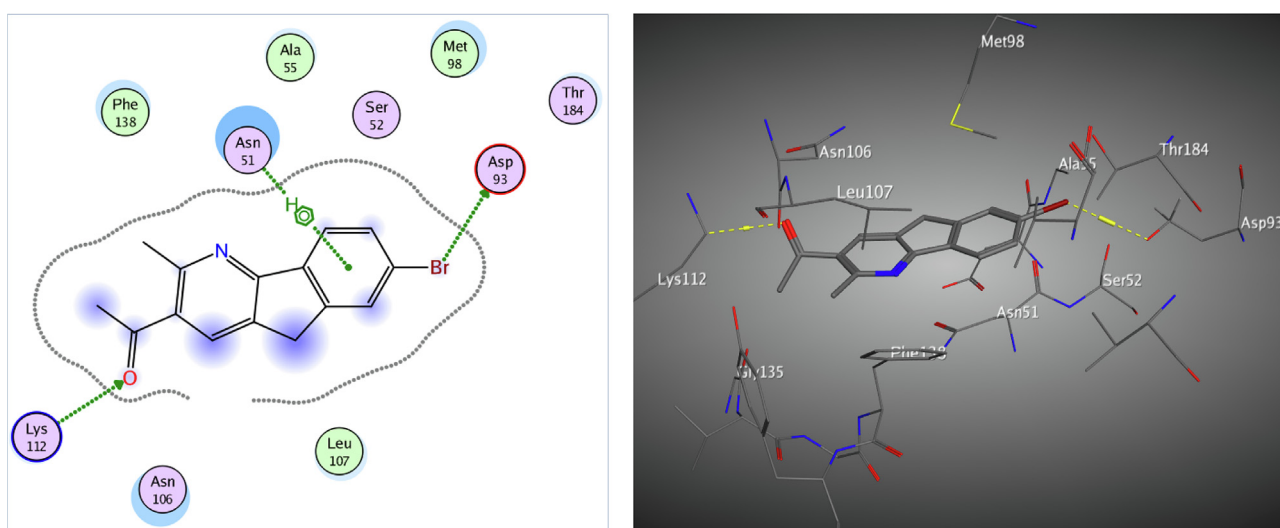
Fig. 8 The 2D and 3D proposed binding modes of **25** inside Hsp90 receptor active site.

served regions and may be accountable for Hsp90 inhibitory activity are (Leu48, Asn51, Ser52, Asp54, Ala55, Lys58, Ile91, Asp93, Gly97, Met98, Asp102, Asn106, Lys112, Gly135, Gly137, Phe138, Val150, Ile151, Thr184, Lys185 and Val186) (Saxena et al., 2010).

Redocking of the co-crystalized ligand was first done for validation. It was found that the carbonyl group was involved in the binding to the key residues; Thr4184 and Gly97 *via* two hydrogen bonds in the active binding site of the Hsp90. Additionally; Asp93 was able to form one H bond with OH group and another C–H bond with the phenyl ring. It displayed docking score = -7.103 kcal/mol and the (RMSD) = 1.05 Å (Fig. 3). The obtained docking results of the most active hits showed their ability to fit in the binding site of the enzyme by a significant number of interactions explaining their potency displayed by both scores and binding poses Table 4, Figs. 4-8. Compounds **8a-c**, **17a**, and **25** were docked perfectly inside the Hsp90 binding site with binding scores = -8.556,

−8.213, −7.982, −8.651, and −7.028 kcal/mol, respectively. Interestingly compounds **8a** and **8b** exhibited similar binding behavior within the active site, where in both compounds Asp93 residue formed hydrogen bond with the phenyl ring of indene moiety, in addition to another hydrogen bond between the NH_2 group on the pyrazolo-pyrimidine scaffold and Gly97.

3. Conclusion

New indene derivatives were developed as Hsp90 inhibitors and their cytotoxicity was assessed on two breast cancer cell lines. Besides, the inhibitory effect of the most active compound was examined on Hsp90 enzyme. Results revealed that **8a** exhibited the most potent cytotoxic effect on MCF7 cell line having IC_{50} = 26.44 ± 4.47 μM with significant inhibitory activity on Hsp90 enzyme with IC_{50} = 18. 79 ± 0.68 nM comparing to reference drug. Furthermore, molecular modeling revealed that **8a** is fitted inside the active site of the enzyme with high score = -8.556 Kcal/mol. On the basis of the obtained

results compound **8a** could be considered as Hsp90 inhibitor, and may be useful for further investigation as a hopeful compound for the development of anti-Hsp90 hits.

4. Experimental

4.1. Instrumentations

Recording melting points	Gallenkamp apparatus
IR spectra	KBr / Pye-Unicam SP300 spectrophotometer
^{1}H and ^{13}C NMR spectra	DMSO d_6 / Varian Gemini 300 NMR spectrometer (300 MHz for ^{1}H NMR and 75 MHz for ^{13}C NMR)
Mass spectra	GCMS-Q1000-EX Shimadzu and GCMS 5988-A HP spectrometers

4.2. Synthesis of 5-bromo-2-((dimethylamino)methylene)-2,3-dihydro-1H-inden-1-one (3)

In 50 mL round flask, we added 0.005 mol of 5-bromo-indan-1-one in 15 mL dry xylene and 0.005 mol of DMF-DMA and the whole mixture was refluxed for 5 h. The progress of the condensation reaction was followed with TLC technique. The colored solid enaminone was collected by filtration and crystalized from ethanol to afford rosy solid, (89 % yield), mp 219–220 °C; IR (KBr) v_{max} 3055 (SP^2 CH), 2917 (SP^3 CH), 1672 (C=O), 1583 (C=C), 1438, 1378, 1201, 1128, 1092, 1057 cm^{-1};^{1}H NMR ((CDCl$_3$) 3.19 (s, 6H, 2CH$_3$), 3.85 (s, 2H, CH$_2$), 7.51(dd, J = 8.5, 0.85 Hz, 1H, Ar-H), 7.54 (s, 1H, =CH), 7.60 (s, H, Ar-H), 7.69 (d, J = 8.5 Hz, 1H, Ar-H). ^{13}C NMR (CDCl$_3$) 31.1 (CH$_3$), 103.6, 124.3, 126.1, 128.4, 130.3, 139.1, 147.5, 149.2, 191.0 (C=O) one carbon overlapped; MS m/z (%): 266 (M$^+$, 26), 256 (83), 264 (23), 235 (55), 208(45), 183 (24), 109 (27), 98 (84), 78 (70), 57 (100). Anal. Calcd. for C$_{12}$H$_{12}$BrNO (266.13): C, 54.16; H, 4.54; N, 5.26. Found: C, 54.03; H, 4.46; N, 5.17 %.

4.3. Reaction of enaminone 3 with heterocyclic amines 4a-d, 13a, b, 18 and 19

Reaction of 0.0025 mol of rosy enaminone **3** with the same number of moles of each of heterocyclic amines **4a-d** or **13a, b** or **18** or **19** in 20 mL acetic acid was refluxed for 5 h. The solid colored product was collected by usual way and washed with ethanol, crystalized with ethanol/dioxane mixture to give a series of indenoazolopyrimidines **8a-d**, **17a,b**, **20** and **21**.

4.3.1. 8-Bromo-3-(phenyldiazenyl)-6H-indeno[2,1-e]pyrazolo[1,5-a]pyrimidin-2-amine (8a)

Dark blue solid, (84 % yield), mp above 300 °C; IR (KBr) v_{max} 3420, 3312 (NH$_2$), 3057 (SP^2 CH), 2952 (SP$_3$ CH), 1592 (C=N), 1437, 1327, 1212, 1035 cm^{-1}; ^{1}H NMR (DMSO d_6) 3.60 (s, 2H, CH$_2$), 7.25 (s, 2H, NH$_2$), 7.35–7.54 (m, 5H, Ar-H), 7.75 (d, J = 8.5 Hz, 1H, Ar-H), 7.82 (s, 1H, Ar-H), 8.01 (d, J = 8.5 Hz, 1H, Ar-H), 8.54 (s, 1H, pyrimdine- H). MS m/z (%): 405 (M$^+$, 31), 402 (24), 389 (100), 375 (74), 326 (66), 299 (43), 274 (22), 190 (18), 84 (63), 77 (32). Anal. Calcd. for C$_{19}$H$_{13}$BrN$_6$ (405.26): C, 56.31; H, 3.23; N, 20.74. Found: C, 56.28; H, 3.05; N, 20.53 %.

4.3.2. 8-Bromo-3-((4-chlorophenyl)diazenyl)-6H-indeno[2,1-e]pyrazolo[1,5-a]pyrimidin-2-amine (8b)

Brown solid, (85 % yield), mp above 300 °C; IR (KBr) v_{max} 3405 (NH$_2$), 1600 (C=N), 1545, 1475, 1373, 1225, 1075 cm^{-1};^{1}H NMR (CDCl$_3$) 3.85 (s, 2H, CH$_2$), 6.54 (s, 2H, NH$_2$), 7.21 (d, J = 8.5 Hz, 2H, Ar-H), 7.51 (d, J = 8.5 Hz, 1H, Ar-H), 7.74 (d, J = 8.5 Hz, 2H, Ar-H),7.83 (s, 1H, Ar-H), 7.92 (d, J = 8.5 Hz, 1H, Ar-H), 8.10 (s,1H, pyrimidine-H); MS m/z (%): 440 (M$^+$, 12), 400 (60), 361 (1), 301 (2), 282 (6), 237 (10), 192 (2), 179 (7), 154 (13), 139 (4), 129 (22), 105 (100), 73 (22). Anal. Calcd. for C$_{19}$H$_{12}$BrClN$_6$ (439.70): C, 51.90; H, 2.75; N, 19.11. Found: C, 51.85; H, 2.67; N, 19.03 %.

4.3.3. 8-Bromo-3-((3-chlorophenyl)diazenyl)-6H-indeno[2,1-e]pyrazolo[1,5-a]pyrimidin-2-amine (8c)

Brown solid, (79 % yield), mp above 300 °C; IR (KBr) v_{max} 3266 (NH$_2$), 1599 (C=N), 1533, 1411, 1351, 1240, 1103, 1051 cm^{-1};^{1}H NMR DMSO d_6) 3.82 (s, 2H, CH$_2$), 7.48–8.22 (m, 7H, Ar-H), 8.37 (s, 2H, NH$_2$), 8.75 (s, 1H, pyrimdine-H).MS m/z (%): 439 (M$^+$, 28), 404 (7), 357 (4), 329 (13), 299 (4), 236 (8), 220 (22), 190 (7), 154 (16), 141 (7), 58 (100), 40 (100).Anal. Calcd. for C$_{19}$H$_{12}$BrClN$_6$ (439.70): C, 51.90; H, 2.75; N, 19.11. Found: 51.83; H, 2.61; N, 19.04 %.

4.3.4. 8-Bromo-3-((2-nitrophenyl)diazenyl)-6H-indeno[2,1-e]pyrazolo[1,5-a]pyrimidin-2-amine (8d)

Brown solid, (82 % yield), mp above 300 °C; IR (KBr) v_{max} 3441, 3210 (NH$_2$), 2936 (SP^3 CH), 1585(C=N), 1434, 1305, 1203, 1039 cm^{-1}; MS m/z (%): 451 (M$^+$, 23), 418 (20), 243 (31), 132 (72), 89 (79), 62 (100), 41 (54). Anal. Calcd. for C$_{19}$H$_{12}$BrN$_7$O$_2$ (450.26): C, 50.68; H, 2.69; N, 21.78. Found: C, 50.51; H, 2.48; N, 21.67 %.

4.3.5. 8-Bromo-3-((2-chlorophenyl)diazenyl)-1H-indeno[2,1-e]pyrazolo[1,5-a]pyrimidin-2(6H)-one (17a)

Dark blue solid, (86 % yield), mp above 300 °C; IR (KBr) v_{max} 3200 (NH), 1691 (C=O), 1533, 1379, 1208, 1096 cm^{-1};^{1}H NMR (DMSO d_6) 3.74 (s, 2H, CH$_2$), 6.95–7.63 (m, 8H, Ar-H and pyridine-H), 8.82 (s, 1H, NH); MS m/z (%): 444 (M$^+$ + 4, 40), 439 (M$^+$, 28), 436 (88), 422 (82), 361 (41), 353 (80), 330 (35), 302 (41), 284 (78), 242 (29), 228 (28), 219 (21), 193 (36), 151 (49), 128 (100), 108 (36). Anal. Calcd. for C$_{19}$H$_{11}$BrClN$_5$O (440.69): C, 51.79; H, 2.52; N, 15.89. Found: C, 51.65; H, 2.42; N, 15.78 %.

4.3.6. 8-Bromo-3-((2-nitrophenyl)diazenyl)-1H-indeno[2,1-e]pyrazolo[1,5-a]pyrimidin-2(6H)-one (17b)

Brown solid, (90 % yield), mp above 300 °C; IR (KBr) v_{max} 3205 (NH), 1736 (C=O), 1502, 1358, 1210, 1150 cm^{-1}; ^{1}H NMR (DMSO d_6) 3.74 (s, 2H, CH$_2$),7.37 (t, J = 8.5 Hz, 1H, Ar-H), 7.62 (s, 1H, Ar-H), 7.87 (s,1H, pyrimidine-H), 7.91 (t, J = 8.5 Hz, 2H, Ar-H), 8.23 (d, J = 8.5 Hz, 1H, Ar-H), 8.28 (d, J = 8.5 Hz, 1H, Ar-H), 8.33 (d, J = 8.5 Hz, 1H, Ar-H),11.61 (s, 1H, NH); MS m/z (%): 450 (M$^+$, 10), 430

(82), 405 (25), 385 (83), 371 (24), 344 (1 0 0), 324 (66), 303 (46), 277 (82), 228 (54), 192 (7). Anal. Calcd. for $C_{19}H_{11}BrN_6O_3$ (451.24): C, 50.57; H, 2.46; N, 18.62. Found: C, 50.64; H, 2.39; N, 18.58 %.

4.3.7. 8-Bromo-6H-indeno[2,1-e][1,2,4]triazolo[1,5-a] pyrimidine (20)

Yellow solid, (90 % yield), mp 290–291 °C; IR (KBr) v_{max} 3057 (SP^2 CH), 2970 (SP^3 CH), 1600 (C=N), 1553, 1437, 1331, 1205, 1035 cm^{-1}; ^1H NMR (DMSO d_6) 3.69 (s, 2H, CH_2), 7.57–7.64 (m,2H), 7.85 (s, 1H, pyrimdine- H), 8.11(s, 1H, Ar-H), 8.41 (s, 1H, triazole-H). ^{13}C NMR (DMSO d_6) 29.79 (CH_2), 124.63, 127.10, 129.77, 130.74, 135.74, 139.35, 144.04, 150.46, 152.49, 160.46, 172.49; MS m/z (%): 287 (M^+, 47), 268 (83), 261 (41), 253 (85), 244 (50), 153 (93), 127 (56), 119 (23), 104 (1 0 0), 63 (33). Anal. Calcd. for $C_{12}H_7BrN_4$ (287.12): C, 50.20; H, 2.46; N, 19.51. Found: C, 50.14; H, 2.39; N, 19.28 %.

4.3.8. 10-Bromo-8H-benzo[4,5]imidazo[1,2-a]indeno[2,1-e] pyrimidine (21)

Dark green solid, (87 % yield), mp 139–140 °C; IR (KBr) v_{max} 1550 (C=N), 1416, 1207, 1049 cm^{-1}; ^1H NMR (DMSO d_6) 3.60 (s, 2H, CH_2), 7.08–7.83 (m, 7H, Ar-H), 8.22 (s, 1H, pyrimdine- H). ^{13}C NMR (DMSO d_6) 31.01 (CH_2), 103.17,113.98, 122.0, 124.22, 124.69, 124.79, 125.40, 128.98, 129.93, 130.34, 130.82, 138.94, 139.76, 147.81, 150.24, 150.55. MS m/z (%): 336 (M^+, 32), 301 (90), 284 (68), 230 (66), 209 (95), 104 (14), 89 (1 0 0). Anal. Calcd. for $C_{17}H_{10}BrN_3$ (336.19); C, 60.74; H, 3.00; N, 12.50. Found: C, 60.62; H, 2.93; N, 12.42 %.

4.4. Reaction of enaminone derivative 3 with active methylene derivatives 22–24

By usual way for the reaction of enaminone with the active methylene, 0.0025 mol of rosy enaminone **3** reacted with active methylene derivatives 22–24 in 20 mL acetic acid in the presence of 0.5 g CH_3COONH_4 with reflux for 5 h. The solid colored product was collected by usual way and washed with ethanol, crystalized with ethanol/dioxane mixture to give a series of indenopyridine derivatives **25–27**.

4.4.1. 1-(7-Bromo-2-methyl-4a,9b-dihydro-5H-indeno[1,2-b] pyridin-3-yl)ethan-1-one (25)

Yellow solid, (88 % yield), mp above 300 °C; IR (KBr) v_{max} 1676 (C=O) 1540, 1251, 1098, 1036 cm^{-1};^1H NMR (CDCl$_3$) 2.19 (s, 3H, CH_3), 2.48 (s, 3H, CH_3), 3.71 (s, 2H, CH_2), 7.53–7.82 (m, 4H, Ar-H and pyridine-H). ^{13}C NMR (CDCl$_3$) 18.35 (CH_3), 24.76 (CH_3), 30.80 (CH_2), 103.46, 116.0, 124.5, 124.8, 126.5, 128.91, 130.81, 131.05, 138.56, 149.23, 154.78, 199.40 (C=O). MS m/z (%): 302 (M^+, 35), 272 (80), 233 (64), 223 (48), 156 (84), 113 (1 0 0), 94 (63), 71 (25).Anal. Calcd. for $C_{15}H_{12}BrNO$ (302.17): C, 59.62; H, 4.00; N, 4.64. Found: C, 59.50; H, 3.91; N, 4.49 %.

4.4.2. 7-Bromo-2-phenyl-5,9b-dihydro-4aH-indeno[1,2-b] pyridine-3-carboxylic acid ethyl ester (26)

Yellow solid, (85 % yield), mp above 300 °C; IR (KBr) v_{max} 3054 (SP^2 CH), 2893 (SP^3 CH), 1679 (C=O), 1579, 1459, 1415, 1375, 1322, 1202, 1108, 1044 cm^{-1};^1H NMR (DMSO d_6) 1.12 (t, J = 8.5 Hz, 3H, CH_3), 3.51 (s, 2H, CH_2), 4.25 (q, J = 8.5 Hz, 2H, CH_2), 6.95–8.13 (m, 9H, Ar-H and pyridine-H). Anal. Calcd. for $C_{21}H_{16}BrNO_2$ (394.26): C, 63.97; H, 4.09; N, 3.55. Found: C, 63.83; H, 4.02; N, 3.43 %.

4.4.3. 7-Bromo-2-oxo-2,4a,5,9b-tetrahydro-1H-indeno[1,2-b] pyridine-3-carboxylic acid ethyl ester (27)

Yellow solid, (84 % yield), mp above 300 °C; IR (KBr) v_{max} 3308 (NH), 1745(C=O), 1691(C=O), 1580, 1416, 1207, 1113, 1046 cm^{-1};^1H NMR (DMSO d_6) 1.30 (t, J = 8.5 Hz, 3H, CH_3), 3.45 (s, 2H, CH_2), 4.35 (q, J = 8.5 Hz, 2H, CH_2), 7.23–8.01 (m, 4H, Ar-H and pyridine-H), 9.94 (s, 1H, NH); Anal. Calcd. for $C_{15}H_{12}BrNO_3$ (334.16): C, 53.91; H, 3.62; N, 4.19. Found: C, 53.78; H, 3.52; N, 4.04 %.

4.5. In vitro cytotoxicity

MTT assay was utilized to explore the cytotoxic behavior of the tested compounds via using a Sigma in vitro MTT-based assay kit. MCF7 and MDA-MB231 breast cancer cell lines were obtained from the American Type Culture Collection, cultured in DMEM medium with penicillin, FBS, and streptomycin at 5 % CO_2 and 37 °C. After treatment with several doses of research compounds, cells were cultured at 37 °C for 48 h, then they were incubated in dark for 4 h with MTT reagent. The absorbance was measured at 560 nm with a plate reader, and cell viability was determined. Finally the IC_{50} values were then calculated.

4.6. Hsp90 inhibitory activity

The inhibitory effect of compound **8a** on the activity of the human heat shock protein 90 ELISA Kit (Cat.No.E3061Hu) was measured. To the standard well, add 50 μl of standard. Then 40 μl of sample should be added to the sample wells, followed by 10 μl of anti-HSP90 antibody and 50 μl of streptavidin-HRP in both the sample and standard wells. Mix well. Apply a sealant to the plate. 60 min at 37 °C of incubation. Remove the sealant, then use a wash buffer to wash the plate five times. For every wash, soak wells in a minimum of 0.35 mL of wash buffer for 30 to 1 min. Aspirate or decant each well for automatic washing, then use wash buffer five times. Place paper towels or another absorbent material nearby to blot the plate. Each well should first receive 50 μl of substrate solution A before receiving 50 μl of substrate solution B. Plate should be incubated for 10 min at 37°Celsius in the dark. Each well's colour will turn to yellow when 50 μl of stop solution is added. Within 10 min of adding the stop solution, measure the optical density of each well using a microplate reader set to 450 nm.

4.7. Molecular docking

In this study, docking was achieved using MOE 2014.09 (MOE, 2014). In order to build structures of the docked compounds, the builder button was used. The tested compounds were docked inside the Hsp90 crystal structure (PDB: 2xjx). To start docking, we used MOE's "Docking" module. Water molecules were deleted throughout the docking steps. The

missing hydrogen atoms were retained to correct ionization states in order to be assigned to the protein structure. The "Ligand Interactions" MOE tool was then used for the analysis of docking results by visualization of the ligand–protein interactions in the active binding site.

Declaration of Competing Interest

The authors declare that they have no known competing financial interests or personal relationships that could have appeared to influence the work reported in this paper.

Appendix A. Supplementary material

Supplementary data to this article can be found online at https://doi.org/10.1016/j.arabjc.2023.104569.

References

Aastha, M., Tanya, P., Tripti, S., 2021. Pyrimidine: a review on anticancer activity with key emphasis on SAR. Future J. Pharm. Sci. 7. https://doi.org/10.1186/s43094-021-00274-8.

Abbas, E.M.H., Farghaly, T.A., Sabour, R., Shaaban, M.R., Abdallah, Z.A., 2022. Design, synthesis, cytotoxicity, and molecular docking studies of novel thiazolyl–hydrazone derivatives as histone lysine acetyl-transferase inhibitors and apoptosis inducers. Arch. Pharm., e2200076 https://doi.org/10.1002/ardp.202200076.

Akira, S., Yukinori, K., Yoshitaka, H., Yoichi, N., Shiro, I., Hideo, B., Yoshito, K., Toshirou, N., Toshihiko, D., 2022. PS4-3 A phase III trial of pimitespib (TAS-116) in patients with advanced gastrointestinal stromal tumor: CHAPTER-GIST-301. Ann. Oncol. 33, S467. https://doi.org/10.1016/j.annonc.2022.05.071.

Alamri, A., Alafnan, A., Huwaimel, B., Abouzied, A.S., Alanazi, J., Alghamdi, A., Alrofaidi, M.A., Alanazi, M.S., Alshehrif, A., Al, H. T., Alobaida, A., Younes, K.M., Farghaly, T.A., 2023. Synthesis of novel series of heterocyclic compounds having two azoles against Methicillin-sensitive Staphylococcus aureus. J. Mol. Struct. 1277,. https://doi.org/10.1016/j.molstruc.2022.134863 134863.

Almehmadi, S.J., Alsaedi, A.M.R., Harras, M.F., Farghaly, T.A., 2021. Synthesis of a new series of pyrazolo[1,5-a]pyrimidines as CDK2 inhibitors and anti-leukemia. Bioorg. Chem. 117,. https://doi.org/10.1016/j.bioorg.2021.105431 105431.

Alsaedi, A.M.R., Farghaly, T.A., Shaaban, M.R., 2022. Fluorinated azole anticancer drugs: synthesis, elaborated structure elucidation and docking studies. Arab. J. Chem. 15,. https://doi.org/10.1016/j.arabjc.2022.103782 103782.

Althagafi, I. I., Abouzied, A. S., Farghaly, T. A., Al-Qurashi, N. T., Alfaifi, M. Y., Shaaban, M. R., Abdel Aziz M. R., 2019. Novel Nano-sized bis-indoline Derivatives as Antitumor Agents J. Heterocyclic Chem., 56, 391-399. DOI 10.1002/jhet.3410

Bayazeed, A., Alenazi, N. A., Alsaedi, A. M.R., Ibrahimd, M. H., Al-Qurashi, N. T., Farghaly, T. A., 2022. Formazan analogous: Synthesis, antimicrobial activity, dihydrofolate reductase inhibitors and docking study Journal of Molecular Structure 1258, 132653. https://doi.org/10.1016/j.molstruc.2022.132653.

Bell, R., Brown, K., 1979. The effects of two "anti-aggressive" compounds, an indenopyridine and benzothiazepin, on shock-induced defensive fighting in rats. Prog. Neuropsychopharmacol. 3, 399–402. https://doi.org/10.1016/0364-7722(79)90053-5.

Berry, D.A., Cronin, K.A., Plevritis, S.K., Fryback, D.G., Clarke, L., Zelen, M., Mandelblatt, J.S., Yakovlev, A.Y., Habbema, J.D.F., Feuer, E.J., 2005. Effect of screening and adjuvant therapy on mortality from breast cancer. N. Engl. J. Med. 353, 1784–1792. https://doi.org/10.1056/NEJMoa050518.

Biebl, M.M., Buchner, J., 2019. Structure, function, and regulation of the Hsp90 machinery. Cold Spring Harb. Perspect. Biol. 11, 1–32. https://doi.org/10.1101/cshperspect.a034017.

Brahmbhatt, D.I., Patel, C.V., Bhila, V.G., Patel, N.H., Patel, A.A., 2015. An efficient synthesis and antimicrobial screening of new hybrid molecules containing coumarin and indenopyridine moiety. Med. Chem. Res. 24, 1596–1604. https://doi.org/10.1007/s00044-014-1228-1.

Chaudhury, S., Meka, P.N., Banerjee, M., Kent, C.N., Blagg, B.S.J., 2021. Structure-based design, synthesis, and biological evaluation of Hsp90β-Selective Inhibitors. Chem. Eur. J. 27, 14747–14764. https://doi.org/10.1002/chem.202102574.

Davies, N.G.M., Browne, H., Davis, B., Drysdale, M.J., Foloppe, N., Geoffrey, S., Gibbons, B., Hart, T., Hubbard, R., Jensen, M.R., Mansell, H., Massey, A., Matassova, N., Moore, J.D., Murray, J., Pratt, R., Ray, S., Robertson, A., Roughley, S.D., Schoepfer, J., Scriven, K., Simmonite, H., Stokes, S., Surgenor, A., Webb, P., Wood, M., Wright, L., Brough, P., 2012. Targeting conserved water molecules: design of 4-aryl-5-cyanopyrrolo[2,3-d]pyrimidine Hsp90 inhibitors using fragment-based screening and structure-based optimization. Bioorg. Med. Chem. 20, 6770–6789. https://doi.org/10.1016/j.bmc.2012.08.050.

El-Shafey, H.W., Gomaa, R.M., El-Messery, S.M., Goda, F.E., 2020. Synthetic approaches, anticancer potential, HSP90 inhibition, multitarget evaluation, molecular modeling and apoptosis mechanistic study of thioquinazolinone skeleton: promising antibreast cancer agent. Bioorg. Chem. 101,. https://doi.org/10.1016/j.bioorg.2020.103987 103987.

Farghaly, T.A., Abdel Hafez, N.A., Ragab, E.A., Awad, H.M., Abdalla, M.M., 2010. Synthesis, anti-HCV, antioxidant, and peroxynitrite inhibitory activity of fused benzosuberone derivatives. Eur. J. Med. Chem. 45, 492–500. https://doi.org/10.1016/j.ejmech.2009.10.033.

Farghaly, T.A., Abdallah, M.A., Masaret, G.S., Muhammad, Z.A., 2015. New and efficient approach for synthesis of novel bioactive [1,3,4] thiadiazoles incorporated with 1,3-thiazole moiety. Eur. J. Med. Chem. 97, 320e333. https://doi.org/10.1016/j.ejmech.2015.05.009.

Farghaly, T.A., Althagafi, I., Ibrahim, M.H., Al-Qurashi, N.T., Farooq, U., 2021. Synthesis under microwaves irradiation, structure elucidation, docking study for inhibiting COVID-19 and DFT calculations of novel azoles incorporated indole moiety. J. Mol. Struct. 1244,. https://doi.org/10.1016/j.molstruc.2021.131263 131263.

Fayed, E.A., Ammar, Y.A., Ragab, A., Gohar, N.A., Mehany, A.B. M., Farrag, A.M., 2020. In vitro cytotoxic activity of thiazole-indenoquinoxaline hybrids as apoptotic agents, design, synthesis, physicochemical and pharmacokinetic studies. Bioorg. Chem. 100,. https://doi.org/10.1016/j.bioorg.2020.103951 103951.

Ghorab, M.M., Alsaid, M.S., 2012. Anticancer activity of novel indenopyridine derivatives. Arch. Pharm. Res. 35, 987–994. https://doi.org/10.1007/s12272-012-0605-x.

Ghorab, M.M., Alsaid, M.S., 2015. Synthesis of some tricyclic indeno [1,2-d] pyrimidine derivatives as a new class of anti-breast cancer agents. Biomed. Res. 26, 422–425.

Gimenez Ortiz, A., Montalar Salcedo, J., 2010. Heat shock proteins as targets in oncology. Clin. Transl. Oncol. 12, 166–173. https://doi.org/10.1007/s12094-010-0486-8.

Kadayat, T.M., Song, C., Kwon, Y., Lee, E.-S., 2015. Modified 2,4-diaryl-5H-indeno[1,2-b]pyridines with hydroxyl and chlorine moiety: Synthesis, anticancer activity, and structure–activity relation-

ship study. Bioorg. Chem. 62, 30–40. https://doi.org/10.1016/j.bioorg.2015.07.002.

Kadayat, T.M., Park, C., Jun, K.-Y., Magar, T.B.T., Bist, G., Yoo, H.Y., Kwon, Y., Lee, E.-S., 2015. Hydroxylated 2,4-diphenyl indenopyridine derivatives as a selective non-intercalative topoisomerase IIα catalytic inhibitor. Eur. J. Med. Chem. 90, 302–314.

Kadayat, T.M., Park, S., Jun, K.-Y., Magar, T.B.T., Bist, G., Shrestha, A., Na, Y., Kwon, Y., Lee, E.-S., 2016. Effect of chlorine substituent on cytotoxic activities: design and synthesis of systematically modified 2,4-diphenyl-5H-indeno[1,2-b]pyridines. Bioorg. Med. Chem. Lett. 26, 1726–1731. https://doi.org/10.1016/j.bmcl.2016.02.053.

Li, L., Wang, L., You, Q.D., Xu, X.L., 2020. Heat shock protein 90 inhibitors: an update on achievements, challenges, and future directions. J. Med. Chem. 63, 1798–1822. https://doi.org/10.1021/acs.jmedchem.9b00940.

Lianos, G.D., Alexiou, G.A., Mangano, A., Mangano, A., Rausei, S., Boni, L., Dionigi, G., Roukos, D.H., 2015. The role of heat shock proteins in cancer. Can. Lett. 360, 114–118. https://doi.org/10.1016/j.canlet.2015.02.026.

Liu, Q., Tu, G., Hu, Y., Jiang, Q., Liu,J., Lin, S., Yu, Z., Li, G., Wu, X., Y., Tang, Huang,X., Xu, J., Liu, Y., Wu, L.. 2022. Discovery of BP3 as an efficacious proteolysis targeting chimera (PROTAC) degrader of HSP90 for treating breast cancer, Eur. J. Med. Chem. 228, 114013 https://doi.org/10.1016/j.ejmech.2021.114013

Molecular Operating Environment (MOE) 2014, Chemical Computing Group Inc., Montreal, Canada http://www.chemcomp.com.

Neckers, L., Mollapour, M., 2015. Heat shock protein 90 and the proteasome: Housekeeping proteins that are also molecular targets for cancer therapy, V. Molecular Basis of Cancer Therapy (Fourth Edition), 779-788.e3. http://dx.doi.org/10.1016/B978-1-4557-4066-6.00056-1

Nguyen, C., La, M.T., Ann, J., Nam, G., Park, H., Park, J.M., Kim, Y., Kim, J.Y., Seo, J.H., Lee, J., 2021. Discovery of a simplified deguelin analog as an HSP90 C-terminal inhibitor, for HER2-positive breast cancer. Bioorg. Med. Chem. Lett. 45,. https://doi.org/10.1016/j.bmcl.2021.128134 128134.

Saxena, A.K., Saxena, S., Chaudhaery, S.S., 2010. Molecular modelling and docking studies on heat shock protein 90 (Hsp90) inhibitors. SAR QSAR Environ. Res. 21, 1–20. https://doi.org/10.1080/10629360903560504.

Sheridan, M.H., 2022. Pimitespib: first approval. Drugs 82, 1413–1418. https://doi.org/10.1007/s40265-022-01764-6.

Shrestha, A., Park, S., Jang, H.J., Katila, P., Shrestha, R., Kwon, Y., Lee, E.-S., 2018. A new phenolic series of indenopyridinone as topoisomerase inhibitors: design, synthesis, and structure-activity relationships. Bioorg. Med. Chem. 26, 5212–5223. https://doi.org/10.1016/j.bmc.2018.09.021.

Taipale, M., Jarosz, D.F., Lindquist, S., 2010. Hsp90 at the hub of protein homeostasis: emerging mechanistic insights. Nat. Rev. Mol. Cell Biol. 11, 515–528. https://doi.org/10.1038/nrm2918.

Whitesell, L., Lindquist, S.L., 2005. Hsp90 and the chaperoning of cancer. Nat. Rev. Canc. 5, 761–772. https://doi.org/10.1038/nrc1716.

Woodhead, A.J., Angove, H., Carr, M.G., Chessari, G., Congreve, M., Coyle, J.E., Cosme, J., Graham, B., Day, P.J., Downham, R., Fazal, L., Feltell, R., Figueroa, E., Frederickson, M., Lewis, J., McMenamin, R., Murray, C.W., O'Brien, M.A., Parra, L., Patel, S., Phillips, T., Rees, D.C., Rich, S., Smith, D., Trewartha, G., Vinkovic, M., Williams, B., Woolford, A.-J.-A., 2010. Discovery of (2,4-Dihydroxy-5-isopropylphenyl)-[5-(4-methylpiperazin-1-ylmethyl)-1,3-dihydroisoindol-2-yl]methanone (AT13387), a Novel Inhibitor of the Molecular Chaperone Hsp90 by Fragment Based Drug Design. J. Med. Chem. 53, 5956–5969. https://doi.org/10.1021/jm100060b.

Zhang, Y., Zhang, T., Li, X., Liang, J., Tu, S., Xu, H., Xue, W., Qian, X., Zhang, Z., Zhang, X., Meng, F., 2021. 2-((1-phenyl-1H-1,2,3-triazol-4-yl)methyl)-2-azabicyclo[1 3.2.1]octan-3-one derivatives: simplification and modification of aconitine scaffold for the discovery of novel anticancer agents. Eur. J. Med. Chem., 210, 1122988. https://doi.org/10.1016/j.ejmech.2020.112988.